



Universiteit
Leiden
The Netherlands

Exome sequencing of ATP1A3-negative cases of alternating hemiplegia of childhood reveals SCN2A as a novel causative gene

Panagiotakaki, E.; Tiziano, F.D.; Mikati, M.A.; Vijfhuizen, L.S.; Nicole, S.; Lesca, G.; ... ; Heinzen, E.L.

Citation

Panagiotakaki, E., Tiziano, F. D., Mikati, M. A., Vijfhuizen, L. S., Nicole, S., Lesca, G., ... Heinzen, E. L. (2023). Exome sequencing of ATP1A3-negative cases of alternating hemiplegia of childhood reveals SCN2A as a novel causative gene. *European Journal Of Human Genetics*, 32, 224-231. doi:10.1038/s41431-023-01489-4

Version: Publisher's Version
License: [Creative Commons CC BY 4.0 license](https://creativecommons.org/licenses/by/4.0/)
Downloaded from: <https://hdl.handle.net/1887/3731513>

Note: To cite this publication please use the final published version (if applicable).

ARTICLE



Exome sequencing of *ATP1A3*-negative cases of alternating hemiplegia of childhood reveals *SCN2A* as a novel causative gene

Eleni Panagiotakaki^{1,24}, Francesco D. Tiziano^{2,24}, Mohamad A. Mikati^{3,24}, Lisanne S. Vijfhuizen⁴, Sophie Nicole⁵, Gaetan Lesca⁶, Emanuela Abiusi⁷, Agnese Novelli⁷, Lorena Di Pietro^{2,7}, I.B.AHC Consortium, IAHCRC Consortium, Aster V. E. Harder^{4,8}, Nicole M. Walley⁹, Elisa De Grandis^{10,11}, Anne-Lise Poulat¹², Vincent Des Portes¹², Anne Lépine¹³, Marie-Cecile Nassogne^{14,15}, Alexis Arzimanoglou¹⁶, Rosaria Vavassori¹⁷, Jan Koenderink¹⁸, Christopher H. Thompson¹⁹, Alfred L. George Jr.¹⁹, Fiorella Gurrieri^{20,21}, Arn M. J. M. van den Maagdenberg^{4,8,25} and Erin L. Heinzen^{22,23,25}

© The Author(s), under exclusive licence to European Society of Human Genetics 2023

Alternating hemiplegia of childhood (AHC) is a rare neurodevelopment disorder that is typically characterized by debilitating episodic attacks of hemiplegia, seizures, and intellectual disability. Over 85% of individuals with AHC have a de novo missense variant in *ATP1A3* encoding the catalytic $\alpha 3$ subunit of neuronal Na^+/K^+ ATPases. The remainder of the patients are genetically unexplained. Here, we used next-generation sequencing to search for the genetic cause of 26 *ATP1A3*-negative index patients with a clinical presentation of AHC or an AHC-like phenotype. Three patients had affected siblings. Using targeted sequencing of exonic, intronic, and flanking regions of *ATP1A3* in 22 of the 26 index patients, we found no ultra-rare variants. Using exome sequencing, we identified the likely genetic diagnosis in 9 probands (35%) in five genes, including *RHOBTB2* ($n = 3$), *ATP1A2* ($n = 3$), *ANK3* ($n = 1$), *SCN2A* ($n = 1$), and *CHD2* ($n = 1$). In follow-up investigations, two additional *ATP1A3*-negative individuals were found to have rare missense *SCN2A* variants, including one de novo likely pathogenic variant and one likely pathogenic variant for which inheritance could not be determined. Functional evaluation of the variants identified in *SCN2A* and *ATP1A2* supports the pathogenicity of the identified variants. Our data show that genetic variants in various neurodevelopmental genes, including *SCN2A*, lead to AHC or AHC-like presentation. Still, the majority of *ATP1A3*-negative AHC or AHC-like patients remain unexplained, suggesting that other mutational mechanisms may account for the phenotype or that cases may be explained by oligo- or polygenic risk factors.

European Journal of Human Genetics (2024) 32:224–231; <https://doi.org/10.1038/s41431-023-01489-4>

INTRODUCTION

Alternating hemiplegia of childhood (AHC) is a rare, early-onset neurodevelopmental disorder with a distinctive clinical presentation, first described in 1971, that involves episodic hemiplegia that can alternate between sides of the body [1]. These individuals may

also have episodes of quadriplegia, paroxysmal attacks of dystonia, abnormal eye movements, and/or autonomic dysfunction, and movement disorders such as chorea, dystonia, and intellectual disability [1–5]. In 2012, de novo variants in *ATP1A3* were found to explain the vast majority (~85%) of cases of AHC, providing

¹Department of Paediatric Clinical Epileptology, Sleep Disorders and Functional Neurology, Member of the ERN EpiCare, University Hospitals of Lyon (HCL), Lyon, France. ²Institute of Genomic Medicine, Catholic University and Policlinico Gemelli, Fondazione Policlinico Universitario Agostino Gemelli IRCSS, Rome, Italy. ³Division of Pediatric Neurology and Developmental Medicine, Duke University, Durham, NC, USA. ⁴Department of Human Genetics, Leiden University Medical Center, Leiden, The Netherlands. ⁵Institute of Functional Genomics, University of Montpellier, CNRS, INSERM, Montpellier, France. ⁶Department of Medical Genetics, University Hospital of Lyon and Claude Bernard Lyon I University, Lyon France - Pathophysiology and Genetics of Neuron and Muscle (PNMG), UCBL, CNRS UMR5261 - INSERM U1315, Lyon, France. ⁷Department of Life Sciences and Public Health, Section of Genomic Medicine, Università Cattolica del Sacro Cuore, Roma, Italy. ⁸Department of Neurology, Leiden University Medical Center, Leiden, The Netherlands. ⁹Department of Pediatrics, Division of Medical Genetics, Duke Health, Durham, NC, USA. ¹⁰Department of Neuroscience, Rehabilitation, Ophthalmology, Genetics, Maternal and Child Health, University of Genoa, Genoa, Italy. ¹¹Child Neuropsychiatry Unit, IRCCS Istituto Giannina Gaslini, Genova, Italy. ¹²Pediatric Neurology Department, Member of the ERN EpiCARE, University Hospitals of Lyon (HCL), Lyon, France. ¹³Service de neuropédiatrie, Centre hospitalo universitaire de la Timone, Marseille, France. ¹⁴Institut des Maladies Rares, Cliniques Universitaires Saint-Luc, UCLouvain, Brussels, Belgium. ¹⁵Service de Neurologie Pédiatrique, Member of the ERN MetabERN, Cliniques Universitaires Saint-Luc, UCLouvain, Brussels, Belgium. ¹⁶Department of Child Neurology and Epilepsy Research Unit, Member of the ERN EpiCARE, Hospital San Juan de Dios, Barcelona, Spain. ¹⁷Euro-Mediterranean Institute for Science and Technology I.E.M.E.S.T., Palermo, Italy. ¹⁸Department of Pharmacology and Toxicology, Radboud University Medical Center, Nijmegen, The Netherlands. ¹⁹Department of Pharmacology, Northwestern University Feinberg School of Medicine, Chicago, IL, USA. ²⁰Department of Medicine, Research Unit of Medical Genetics, Università Campus Bio-Medico di Roma, Roma, Italy. ²¹Operative Research Unit of Medical Genetics Fondazione Policlinico Universitario Campus Bio-Medico, Roma, Italy. ²²Division of Pharmacology and Experimental Therapeutics, Eshelman School of Pharmacy, University of North Carolina at Chapel Hill, Chapel Hill, NC, USA. ²³Department of Genetics, School of Medicine, University of North Carolina at Chapel Hill, Chapel Hill, NC, USA. ²⁴These authors contributed equally: Eleni Panagiotakaki, Francesco D. Tiziano, Mohamad A. Mikati. ²⁵These authors jointly supervised this work: Arn M. J. M. van den Maagdenberg, Erin L. Heinzen. Lists of members and their affiliations appears in the Supplementary Information. ✉email: A.M.J.M.van_den_Maagdenberg@lumc.nl; eheinzen@unc.edu

Received: 1 August 2023 Revised: 25 September 2023 Accepted: 18 October 2023

Published online: 14 December 2023

evidence of the early clinical hypotheses that suggested a distinct monogenic phenotype [6, 7]. Still, a number of patients who fulfill the clinical diagnostic criteria of AHC remain genetically unexplained. As comprehensive sequencing of the coding regions of *ATP1A3* had not identified a causal mutation, these cases are referred to as *ATP1A3*-negative, either typical AHC patients or patients with one or more of the hallmark clinical traits observed in the condition (AHC-like). Exome sequencing in parallel studies has shown that rare protein-disrupting variants in *ATP1A2* [8, 9] and *RHOBTB2* [10, 11] contribute to AHC, although these collectively explain a very small fraction of cases. Hence we here sought to (1) use targeted whole-gene sequencing of *ATP1A3* to look for non-coding pathogenic variants in our cohort of 26 *ATP1A3*-negative patients, and (2) use exome sequencing to further identify other genes that may be responsible for the observed phenotypes.

MATERIALS (SUBJECTS) AND METHODS

Study participants

Twenty-six individuals with typical AHC (or AHC-like) were consented and enrolled at either Duke University, University Hospitals of Lyon, Catholic University in Rome, or Leiden University Medical Center. Unaffected parents were also collected for 20 of the probands (Table 1). Seventeen probands were sporadic, one proband had two additional affected full siblings (quintet), one proband had one affected sibling (quad), and one proband had an affected half-sibling (Fig. 1). Probands were classified as “typical” if they fulfilled the diagnostic criteria [2]. In all cases, only one affected child underwent targeted gene or exome sequencing. DNA was extracted from blood or saliva from the proband and unaffected parents for genomic analyses at the referral Centers. A control cohort consisted of 11,151 individuals sequenced as part of other genetics studies in the Institute for Genomic Medicine (Columbia University, New York, NY, USA) was used to exclude site-specific artifacts and ascertain variant frequency in the population. This cohort consisted of healthy individuals or individuals with phenotypes unrelated to neurodevelopmental disorders.

Following the analysis of the exome sequence data, two additional *ATP1A3*-negative AHC cases (IT06 and 13A2344) were identified with rare missense *SCN2A* variants. These individuals were sequenced and analyzed as part of other studies. Since they were not analyzed as part of the initial cohort, these are being reported as secondary findings. Phenotypic information based on presence or absence of the six core features of AHC [2] is provided for all probands and affected family members ($n = 32$) (Supplementary Table 1).

Targeted and exome sequencing and data processing

DNA samples from all 26 probands and parents underwent exome sequencing using either the IDT xGen Exome Research Panel v1 (IDT Corporation, Newark, New Jersey, USA) or the Nimblegen SeqCap EZ V3.0 Exome Enrichment Kit (NimbleGen Systems GmbH, Pleiskirchen, Germany) per protocol. A subset of 22 probands also underwent targeted sequencing on a custom-designed panel (Nimblegen SeqCap EZ V3.0 Custom Enrichment Kit; NimbleGen Systems GmbH, Pleiskirchen, Germany) that included the full gene sequence of *ATP1A3*, including protein-coding, non-coding, and 1 kb up- and downstream of the protein-coding sequence. The other four samples from the exome-sequenced cohort did not have sufficient DNA available for such targeted deep sequencing of *ATP1A3*. Sequencing was performed on the HiSeq2500 and NovaSeq platforms (Illumina, Inc., San Diego, CA, USA). The sequenced fragments were aligned with DRAGEN to hg19/GRCh37. Variants were called using the Genome Analysis Toolkit (GATK) v3.6 best practices [12]. Variants were annotated using consensus coding sequence (release 20) using snpEff [13]. Genomic analyses were performed using Analysis Tool for Annotated Variants [14].

Two additional cases with an *SCN2A* variant were identified separately from the 26 exome-sequenced probands. One case harboring the de novo variant in *SCN2A* underwent exome sequencing at Catholic University in Rome using the Ion AmpliSeq™ Exome RDY Kit (Thermo Fisher Scientific, Waltham, MA, USA) according to the manufacturer’s instructions. Sequencing was performed by the ION-Proton Instrument (Thermo Fisher Scientific, Waltham, MA, USA). Raw data were aligned to the hg19 by the Torrent Suite (v.5.0.4). Following the upload of the BAM file into the Ionreporter cloud tool, variants were identified by the Variant Caller Plugin (v. 5.10). The second individual, who was found to have an *SCN2A* variant, underwent targeted sequencing using a custom Nimblegen SeqCap EZ V3.0 Custom Enrichment Kit (NimbleGen Systems GmbH, Pleiskirchen, Germany) that included the protein-coding regions of *SCN2A*. Parental DNA was unavailable in this case to ascertain inheritance.

Calling of rare variants and genotypes from exome and target sequencing in probands

De novo variants were identified from the annotated variant lists using the following criteria: (1) heterozygous variant call in the proband with at least 10-fold coverage; (2) exclude variants with a minor allele frequency (MAF) > 0% in the Institute of Genomic Medicine control cohort, and in Exome Variant Server (EVS), Exome Aggregate Consortium (ExAC release 0.3), and gnomAD browser (v2.1.1); (3) exclude variants with a GATK RMSMappingQuality score of < 40, QualbyDepth Score < 2, quality score < 50; (4) exclude variants with a variant allele fraction of < 30% and < 70%; (5) exclude variants in RepeatMasker regions (RepeatMasker 4.1.0, <http://www.repeatmasker.org>); (6) in cases where sequencing of unaffected was performed, the parents were required to have a homozygous reference genotype with at least 10-fold coverage; and (7) for exome sequence analysis, we further limited de novo variant calls only to those predicted to modify the function or amount of protein [missense (PolyPhen2 probably/possibly damaging), variants in conserved splicing regions (variant at the exon-intron boundary within 3 bases into an exon or 8 bases into the intron), nonsense, or indels]. Given the high rate of false positives when the variant allele fractions were < 30%, we only evaluated known pathogenic variants and any variant in *ATP1A3* with variant allele fractions < 30% to consider the possibility of mosaicism for the gene-negative AHC cases. The list of de novo variants is provided in Supplementary Table 2.

We also compiled rare hemizygous and homozygous genotypes from each of the probands using the following criteria: (1) homozygous or hemizygous genotype in the proband with at least 10-fold coverage; (2) exclude genotypes at variants sites with MAF < 0.5% in any population subset and homozygous and/or hemizygous genotype frequency > 0 among internal controls or any population in EVS, Exome Aggregate Consortium (ExAC release 0.3), and gnomAD browser (v2.1.1); (3) exclude variants with a GATK RMSMappingQuality score of < 40 and a GQ score of < 20 in the proband; (4) exclude genotypes in the proband with a variant allele fraction of < 80%; (5) exclude variants in RepeatMasker regions; (6) in cases where sequencing of unaffected was performed, both parents were required to have 10-fold coverage at the variant site and the mother was required to be heterozygous for hemizygous candidates in the proband, and both mother and father were required to be heterozygous for homozygous candidates in the proband; (7) for exome sequence analysis, we further limited homozygous and hemizygous variant calls only to those predicted to modify the function or amount of protein [missense (PolyPhen2 probably/possibly damaging), variants in conserved splicing regions (variant at the exon-intron boundary within 3 bases into an exon or 8 bases into the intron), nonsense, or indels]. The list of candidate homozygous and hemizygous genotypes in the probands is provided in Supplementary Table 2.

Table 1. Study cohort.

| family ID | subject ID | phenotype | gender | trio | affected family members | genomic analysis | % of full <i>ATP1A3</i> gene ^a | % of protein-coding regions of <i>ATP1A3</i> ^b |
|------------|-----------------------|-----------|--------|------------------|--|---------------------------|---|---|
| ahcbh | ahcduplicatepi4538bh1 | atypical | female | yes | no | exome/targeted sequencing | 97.44 | 97.8 |
| ahcbv | ahcduplicatepi4542bv1 | atypical | female | no, proband only | no | exome/targeted sequencing | 99.82 | 98.7 |
| ahcaw | ahcduplicatepi2937aw1 | atypical | female | yes | no | exome/targeted sequencing | 98 | 96.1 |
| ahcn | ahcduplicatepi3911n4 | atypical | female | yes | yes, affected half-sibling (same mother) | exome/targeted sequencing | 95.54 | 98.7 |
| ahcbj | ahcduplicatepi4512bj1 | atypical | female | yes | no | exome/targeted sequencing | 91.33 | 98.2 |
| ahcbw | ahcduplicatepi4542bw1 | atypical | male | no, proband only | no | exome/targeted sequencing | 99.41 | 98.7 |
| ahcao | ahcduplicatepi3905ao1 | atypical | male | yes | no | exome/targeted sequencing | 94.83 | 96.6 |
| ahcbz | ahc14A84bz1 | typical | female | yes | no | exome/targeted sequencing | 98.96 | 98.6 |
| ahcbi | ahcduplicatepi4529bi1 | typical | female | yes | no | exome/targeted sequencing | 97.85 | 98.7 |
| ahcbd | ahcduplicatepi4588bd1 | typical | female | yes | no | exome/targeted sequencing | 97.66 | 98.7 |
| ahcx | ahcduplicatepi3902x1 | typical | female | no, proband only | no | exome/targeted sequencing | 96.98 | 98.5 |
| ahcbb | ahcduplicatepi3937bb1 | typical | female | no, proband only | no | exome/targeted sequencing | 97.84 | 98.3 |
| ahcbs | ahcduplicatepi4542bs1 | typical | female | no, proband only | no | exome/targeted sequencing | 99.99 | 98.7 |
| ahcaa | ahc13A3478aa1ex | typical | female | yes | no | exome/targeted sequencing | 99.74 | 98.7 |
| ahcby | ahc150010by1 | typical | female | yes | no | exome/targeted sequencing | 99.04 | 98.2 |
| dukepi4547 | ahcduplicatepi4547bf4 | typical | male | yes | three additional affected full siblings | exome/targeted sequencing | 97.22 | 98.7 |
| ahcbo | ahcduplicatepi4524bo1 | typical | male | yes | no | exome/targeted sequencing | 97.68 | 97.9 |
| ahcbc | ahcduplicatepi4593bc1 | typical | male | yes | no | exome/targeted sequencing | 97.08 | 98.7 |
| ahcad | ahc13A1635ad1ex | typical | male | yes | no | exome/targeted sequencing | 99.5 | 98.7 |
| ahcab | ahc13A2107ab1ex | typical | male | yes | no | exome/targeted sequencing | 99.03 | 98.2 |
| ahcag | ahc13A581ag1ex | typical | male | yes | no | exome/targeted sequencing | 98.77 | 98.7 |
| ahcah | ahc157184ah1ex | typical | male | no, proband only | no | exome/targeted sequencing | 99.29 | 98.7 |

Table 1. continued

| family ID | subject ID | phenotype | gender | trio | affected family members | genomic analysis | % of full <i>ATP1A3</i> gene ^a | % of protein-coding regions of <i>ATP1A3</i> ^b |
|--------------------|-------------------|-----------|--------|------------------|--------------------------------------|-------------------------------------|---|---|
| ahcbe | ahcdukeepi4580be1 | atypical | female | yes | one additional affected full sibling | exome | NA | 98.7 |
| ahcav | ahcit01ap1 | typical | female | yes | no | exome | NA | 98.7 |
| ahci | ahc149666i1 | typical | female | yes | no | exome | NA | 98.7 |
| ahck | ahcchc2k1 | typical | female | yes | no | exome | NA | 98.7 |
| ahcac ^c | ahc13A2344ac1 | typical | male | no, proband only | no | targeted sequencing of <i>SCN2A</i> | NA | NA |
| IT06 ^c | IT06 | typical | female | no, proband only | no | exome | NA | NA |

NA not applicable.

^aSequenced at least 10-fold in proband.

^bSequenced at least 10-fold in proband (exome and targeted sequencing sequencing).

^cCases identified after original sequencing study.

Finally, compound heterozygous genotypes from the proband were compiled by first compiling all qualifying heterozygous variant calls that included (1) heterozygous variant call in the proband with at least 10-fold coverage; (2) exclude variants with MAF > 0.5% in the Institute of Genomic Medicine control cohort, and in EVS, Exome Aggregate Consortium (ExAC release 0.3), and gnomAD browser (v2.1.1); (3) exclude variants with a GATK RSMMappingQuality score of <40, QualbyDepth Score <2, quality score <50; (4) exclude variants with a variant allele fraction of <30% and <70%; (5) exclude variants in RepeatMasker regions; and (6), for exome sequence analysis, we further limited candidate de novo variant calls only to those predicted modify the function or amount of protein [missense (PolyPhen2 probably/possibly damaging), variants in conserved splicing regions (variant at the exon-intron boundary within 3 bases into an exon or 8 bases into the intron), nonsense, or indels].

Compound heterozygous genotypes were only evaluated in trios where we could confirm bi-allelic inheritance. The list of compound heterozygotes in the probands is provided in Supplementary Table 2.

Variants were assessed for pathogenicity using the principles outlined by the American College of Medical Genetics (ACMG) [15].

Functional evaluation of *ATP1A2* variants

Human Na⁺/K⁺-ATPase α 2 subunit cDNA was subcloned as previously described [16]. In brief, to distinguish endogenous Na⁺/K⁺-ATPase activity from that of transfected Na⁺/K⁺-ATPase, two additional mutations were introduced in the original α 2 subunit cDNA to express an ouabain-resistant isoform. Next, FHM2 missense variants p.E332Q and p.M813K were introduced into the ouabain-resistant wild-type α 2 subunit construct by site-directed mutagenesis. All constructs were sequence verified.

HeLa cells (5×10^5) were transfected with 1.6 μ g plasmid DNA using Lipofectamine 2000 Transfection Reagent in Opti-Mem medium (Invitrogen, Waltham, MA, USA) and cultured in DMEM-containing Glutamax and 10% FCS. Two days after transfection, one-third of the cells were seeded on 10-cm petri dishes and after 5 days of ouabain (1 μ M) challenge, colonies were stained with 1% methylene blue in 70% methanol, scanned, and analyzed with ImageJ (NIH and LOCI, University of Wisconsin, WI, USA). Each transfection was performed three times in triplicates. Two days after transfection, two-thirds of the cells were harvested for Western blot analysis as described previously [16]. The α 2 subunit-specific polyclonal antibody HERED was used for staining [17]. The blot was incubated with the secondary antibody goat anti-rabbit Alexa FluorTM 680 (Abcam, Cambridge, UK) and scanned, with the Odyssey Imaging System (LI-COR Biosciences, Lincoln, NE, USA).

Functional evaluation of *SCN2A* variants

HEK293T cells stably transfected with the human sodium channel β 1 (*SCN1B*) and β 2 (*SCN2B*) auxiliary subunits (HEK-beta cells) were maintained in Dulbecco's modified Eagle's medium (GIBCO/Invitrogen, San Diego, CA, USA) supplemented with 10% fetal bovine serum (Atlanta Biologicals, Norcross, GA, USA), 2 mM L-glutamine, 50 units/mL penicillin, and 50 μ g/mL streptomycin at 37 °C in 5% CO₂. For automated electrophysiology experiments, full-length WT or variant *SCN2A* (Na_v1.2) cDNA was electroporated into HEK-beta cells using the MaxCyte STX electroporation system (MaxCyte Inc., Gaithersburg, MD, USA). Automated patch clamp recording was performed using the Nanion Sycropatch 768PE platform (Nanion Technologies, Munich, Germany) using single-hole low resistance (3–4 M Ω) recording chips. Pulse generation and data collection were performed using PatchControl384 v1.6.6 and DataControl384 v1.6.0 software (Nanion Technologies, Munich, Germany). Whole-cell currents were acquired at 10 kHz, series resistance was compensated 80%, and leak currents were subtracted using P/4 subtraction. The external solution contained (in mM): 140 NaCl, 4 KCl, 2 CaCl₂, 1 MgCl₂, 1 HEPES, 5 glucose, with the final pH adjusted to 7.4 with NaOH, and osmolality adjusted to

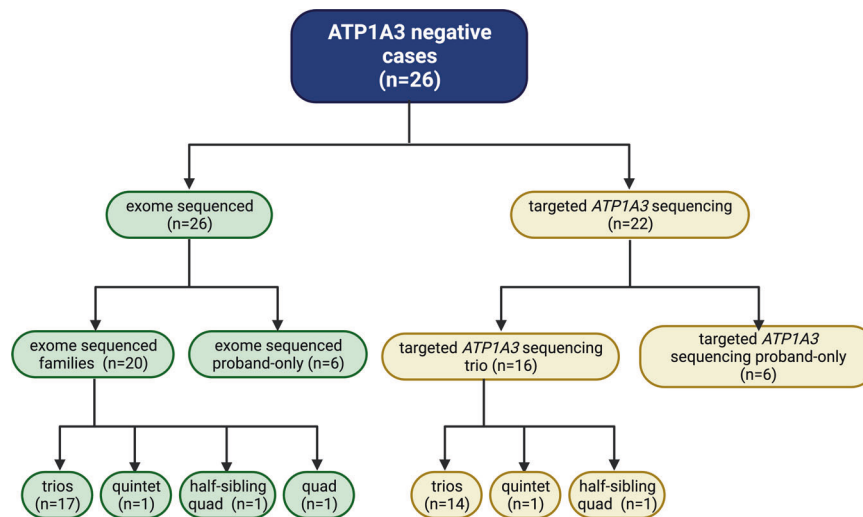


Fig. 1 Cohort overview. Cohort breakdown for individuals undergoing exome ($n = 26$, green shading) and targeted ($n = 22$, yellow shading) sequencing of *ATP1A3*. Exome and panel sequenced cohorts are further subdivided into cases where familial samples were available and proband-only cases.

300 mOsm/kg/L with sucrose. The composition of the internal solution was (in mM): 110 CsF, 10 CsCl, 10 NaCl, 20 EGTA, 10 HEPES, with the final pH adjusted to 7.2 with CsOH, and osmolality adjusted to 300 mOsm/kg/L with sucrose. High-resistance seals were obtained by addition of seal enhancer solutions, which was comprised of (in mM): 80 NaCl, 3 KCl, 35 CaCl₂, 10 MgCl₂, 10 HEPES, with the final pH adjusted to 7.4 with NaOH. Prior to recording, cells were washed twice with external solution, and the final concentrations of CaCl₂ and MgCl₂ were 3 mM and 2 mM, respectively. Biophysical data were collected only from cells with currents larger than -200 pA. Stringent criteria were set to select cells included in the final analysis seal resistance ≥ 200 M Ω , access resistance ≤ 20 M Ω , capacitance ≥ 2 pF, and sodium reversal potential between 45 and 85 mV. Voltage control was assessed from conductance-voltage (GV) curves and cells were included in the final analysis if two adjacent points on the GV curve showed no more than a 7-fold increase. Unless otherwise noted, all chemicals were obtained from SigmaAldrich (St. Louis, MO, USA). Data were analyzed and plotted using a combination of DataControl384 v1.6.0 (Nanion Technologies, Munich, Germany), Clampfit 10.4 (Molecular Devices, San Jose, CA, USA), Microsoft Excel (Microsoft Office 2019, Redmond, WA, USA), and GraphPad Prism (GraphPad Software, San Diego, CA, USA). Whole-cell currents were normalized to membrane capacitance, and data are expressed as mean \pm SEM unless otherwise noted. One-way ANOVA with Dunn's *post hoc* test was used for statistical comparison, and the threshold for statistical significance was $P \leq 0.05$.

RESULTS

Analysis of *ATP1A3*

The protein-coding sequencing from both targeted and exome sequencing of *ATP1A3* in the 26 probands was nearly complete with 98% of protein-coding exons sequenced at least 10-fold on average (min. 96%) (Table 1). Across all of the 22 individuals undergoing targeted sequencing, we identified no mosaic or germline de novo variants in protein-coding or non-coding regions in leukocyte-derived DNA. We also found no homozygous or compound heterozygous *ATP1A3* variants in any of the cases.

Exome sequence analysis

De novo variants. A total of 31 protein-coding putatively functional de novo variants were identified in the 20 trios who underwent exome sequencing. Only one gene, *RHOBTB2*, had de

novo variants in multiple individuals with three individuals having three different missense variants. Observing three de novo variants in three different individuals accounting for gene size, sequence mutability is highly unlikely to occur by chance (FitDNM, $P = 1.3 \times 10^{-11}$) [18]. Even correcting for all of the 18 K genes using a Bonferroni correction, the enrichment is still significant.

American College of Medical Genetics and Genomics (ACMG) diagnostic analysis. In addition to the three likely pathogenic variants in *RHOBTB2*, we also identified pathogenic or likely pathogenic de novo variants in additional probands in *ATP1A2* ($n = 1$), *ANK3* ($n = 1$), *CHD2* ($n = 1$), and *SCN2A* ($n = 1$). The de novo variant in *CHD2* was identified in a family with two affected children, however, the other affected child did not carry the *CHD2* variant. Clinically, the *CHD2* variant was deemed to be pathogenic and partially contributing to the phenotype of the proband. Overall, no pathogenic or likely pathogenic compound heterozygous variant sets or homozygous or newly hemizygous variants were identified.

One variant of unknown significance was identified in the exome sequence data, a stop-gained variant *RHOBTB2* that was inherited from an unaffected father (Table 2, Supplementary Table 2).

Phenotyping and functional characterization

RHOBTB2: In total, we identified three likely pathogenic variants and one variant of unknown significance (VOUS) in *RHOBTB2* (Table 2). Two of the cases with a genetic diagnosis presented with typical AHC (ahc13A581ag1 ex and ahcahc2k1) while one presented atypically lacking obvious bouts of hemiplegia or quadriplegia (ahcdukeepi4538bh1). The case with the stop gained VOUS (ahcdukeepi4542bv1) also presented atypically with unclear information regarding bouts of hemiplegia or quadriplegia (Supplementary Table 1).

ATP1A2: Among the exome-sequenced cases, we identified three rare variants in *ATP1A2*, including one likely pathogenic de novo variant, one likely pathogenic variant with unknown inheritance, and one likely pathogenic splice site variant in *ATP1A2* inherited from a father who is diagnosed with hemiplegic migraine. Only the likely pathogenic variant with unknown inheritance presented with an atypical presentation with no reports of quadriplegia or relief from hemiplegic attacks upon sleeping (ahcdukeepi4542bw1, Supplementary Table 1). None of the three probands were deemed

Table 2. Candidate genetic diagnoses in *ATP1A3*-negative AHC cohort.

| Sample ID | Inheritance | Variant ID (chr-position-ref-alt, hg19) | Variant Type | GeneName | Transcript | HGVS_c | HGVS_p | ACMG classification |
|--------------------------------|--|---|--------------|----------------|-----------------|-------------------|------------|---------------------|
| ahc1496661 | de novo | 10-62023779-C-T | snv | ANK3 | ENST00000280772 | c.514-1 G > A | NA | likely pathogenic |
| ahc14A84bz1 | de novo | 1-160097587-G-C | snv | <i>ATP1A2</i> | ENST00000361216 | c.994 G > C | p.E332Q | likely pathogenic |
| ahcdukeepi4542bw1 ^a | inheritance unknown | 1-160105782-T-A | snv | <i>ATP1A2</i> | ENST00000361216 | c.2438 T > A | p.M813K | likely pathogenic |
| ahcdukeepi4524bo1 ^a | inherited from father with hemiplegic migraine | 1-160097615-G-A | snv | <i>ATP1A2</i> | ENST00000361216 | c.1017 +5 G > A | NA | likely pathogenic |
| ahcdukeepi4580be1 | de novo | 15-93540315-GAA-G | indel | <i>CHD2</i> | ENST00000394196 | c.3722_3723delAA | p.E1241fs | likely pathogenic |
| ahc13A581 ag1ex | de novo | 8-22864414-C-T | snv | <i>RHOBTB2</i> | ENST00000251822 | c.656 C > T | p.S219F | likely pathogenic |
| ahcahc2k1 | de novo | 8-22861984-G-A | snv | <i>RHOBTB2</i> | ENST00000251822 | c.37 G > A | p.E13K | likely pathogenic |
| ahcdukeepi4538bh1 | de novo | 8-22865140-G-A | snv | <i>RHOBTB2</i> | ENST00000251822 | c.1382 G > A | p.R461H | pathogenic |
| ahcdukeepi4542bv1 | inherited from unaffected father ^c | 8-22862900-C-T | snv | <i>RHOBTB2</i> | ENST00000251822 | c.208 C > T | p.R70* | VOUS |
| ahcdukeepi4593bc1 | de novo | 2-166237628-CAGA-C | indel | <i>SCN2A</i> | ENST00000283256 | c.4477_4479delGAA | p.E1493del | pathogenic |
| IT06 ^b | de novo | 2-166245267-T-G | snv | <i>SCN2A</i> | ENST00000283256 | c.4951 T > G | p.F1651V | likely pathogenic |
| ahc13A2344ac1 ^b | unknown | 2-166243356-A-G | snv | <i>SCN2A</i> | ENST00000283256 | c.4652 A > G | p.E1551G | likely pathogenic |

Indel insertion -deletion, snv single nucleotide variation, NA non applicable.

^aPatient previously reported in Moya-Mendez et al (2021) [19].

^bVariants identified in separate studies (see Materials and Methods).

^cInherited determined from clinical sequencing; VOUS variant of unknown significant.

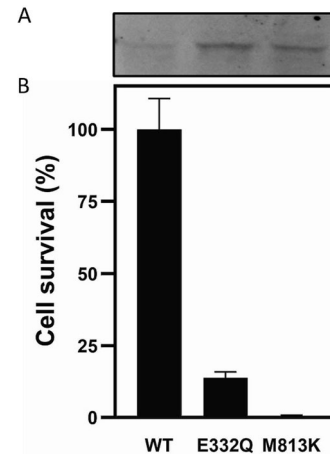


Fig. 2 Ouabain-survival assay in transfected HeLa cells. **A** Western blot analysis of HeLa cells transfected with wild-type (WT) or *ATP1A2* variant cDNA. (anti-HERED antibody). **B** Ouabain sensitivity as determined by cell survival of cells transfected with either wild-type or *ATP1A2* cDNA variants. Bars represent cell survival after 5 days of ouabain treatment ($n=3$). Error bars show standard error of the mean. WT, p.E332Q, and p.M813K, studied variants. The glutamate residue at position 332 is part of the ion-binding pocket of the Na^+/K^+ -ATPase [30]. Structural effects of replacing glutamic acid with glutamine (E332Q) can lead to a minor conformational shift of the amino acid, disrupting the binding pocket resulting in the observed decrease in cell survival. The methionine residue at position 813 is located in the sixth transmembrane domain, close to cation-binding amino acid aspartate 808. Replacement of this amino acid with the positively charged lysine most likely disturbs the binding pocket in such a way that in our assay cell survival is decreased to zero.

clinically to have hemiplegic migraine (Supplementary Table 1). We note that two of the individuals with likely pathogenic *ATP1A2* variants (ahcdukeepi4542bw1 and ahcdukeepi4524bo1) were reported in a previous publication [19] and reported to have an epileptic encephalopathy in addition to having clinical presentations consistent with AHC. In vitro functional evaluation of p.E332Q and p.M813K demonstrated that the expression levels were comparable or higher than that of the wild-type, whereas cell survival was decreased to 14% and 0%, respectively (Fig. 2). This indicates that both variants have functional consequences on sodium-potassium pump functioning and can be considered pathogenic. Consistent with these in vitro functional findings, a previous publication reported AHC-like phenotypes in an M813K mouse model [19].

SCN2A: In addition to the identification of the in-frame de novo *SCN2A* indel (p.E1493del) in one of the patients included in this study, we had identified (likely) pathogenic rare missense variants (p.E1551G, p.F1651V) in two additional cases that met the AHC criteria prior to the initiation of this study. One of the newly identified *SCN2A* variants was de novo and the other was of unknown inheritance (parental samples were not available). In vitro functional evaluation of all three variants demonstrated varying patterns of dysfunction (Fig. 2; Supplemental Table 3). The de novo *SCN2A* indel variant exhibited current density that was not significantly different from background (endogenous) indicating a complete loss-of-function. By contrast, the two missense variants were functional but had significantly altered properties including depolarized voltage-dependence of steady-state inactivation, slower time course of fast inactivation, significantly enhanced channel activation during a slowly depolarizing voltage ramp (p.E1551G only), slower recovery from inactivation and greater loss of activity with repeated depolarizations. These functional features support the pathogenicity of the *SCN2A* variants.

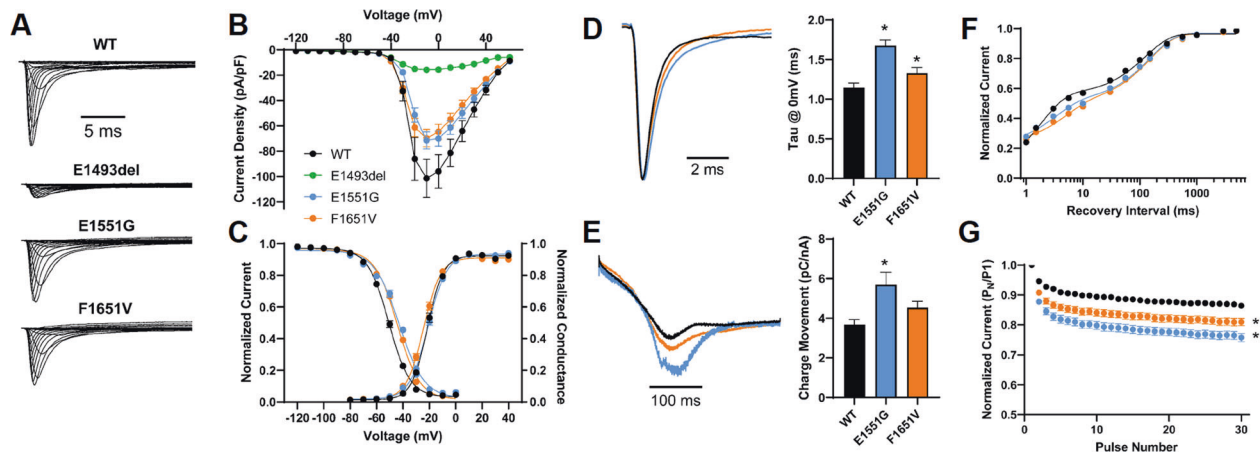


Fig. 3 Functional properties of AHC2-associated *SCN2A* variants. **A** Average whole-cell sodium currents normalized to peak current of the wild-type (WT) channel. **B** Current-voltage relationships. **C** Voltage-dependence of activation and inactivation. **D** Average normalized whole-cell sodium currents elicited at 0 mV, and summary data showing time-constant of fast inactivation. **E** Average normalized whole-cell ramp currents normalized to wild-type current and summary data showing charge movement elicited by the voltage ramp. **F** Time course of recovery from inactivation. **G** Frequency dependent run down of peak current at 20 Hz. All data are expressed as mean \pm SEM with 28 to 120 cells per group for panels **A–C, F, G**, and 12–42 cells per group for (**D** and **E**). Color coding is shown in (**B**). Asterisks indicate $P < 0.05$ for differences between variant and wild-type *SCN2A*.

DISCUSSION

In this study, we sought to determine the genetic cause of 26 unrelated probands with AHC or an AHC-like phenotype with no previously identified molecular diagnosis. Comprehensive (intronic, exonic, and 1-kb flanking regions) and exome sequencing of the *ATP1A3* gene found no evidence of overlooked *ATP1A3* variants. However, likely genetic diagnoses were identified in 11 probands (42%) in five genes, including *RHOBTB2* ($n = 3$), *ATP1A2* ($n = 3$), *ANK3* ($n = 1$), *SCN2A* ($n = 3$), and *CHD2* ($n = 1$). Each of these genes has been previously associated with neurodevelopmental (or neurological) disorders [16, 20], and two (*RHOBTB2* and *ATP1A2*) have been specifically implicated in AHC or AHC-like presentations [9, 11, 21]. These observations are consistent with several isolated case reports of AHC or AHC-like presentations in individuals with likely pathogenic variants in neurodevelopmental disorder genes not classified as AHC genes (*cf.* Panagiotakaki et al. 2023) [20].

ATP1A2 was first associated in 2004 when a rare variant was found to co-segregate in a large multiplex family with AHC and familial hemiplegic migraine [8]. Mutations in *ATP1A2* are, however, most commonly known to cause hemiplegic migraine type 2 [22], a rare autosomal dominant severe form of migraine with aura [23]. In hemiplegic patients, the aura consists of transient motor weakness varying from mild paresis to hemiplegia. There is overlap in the phenotypic spectrum between hemiplegic migraine and AHC [8, 24] based on clinical similarities of the attacks and the paroxysmal nature of both disorders. A distinction can be made based on choreoathetosis, dystonic posturing, and a progressive course associated with intellectual disability [2, 21, 25]. Our genetic findings, coupled with functional analyses supporting pathogenicity, further solidify the association of *ATP1A2* in AHC.

RHOBTB2 likewise was previously associated with AHC and AHC-like presentations [11]. In that study [11], 11 affected patients were described all with rare heterozygous missense variants in exon 9; in nine patients it was possible to assess the parent of origin and it was found that the variants had originated de novo. Two out of three of the likely pathogenic variants in *RHOBTB2* identified in this study were located in exon 9 (exon 5 of the protein-coding sequence) (Table 2). The majority of our cases had presentations that met the criteria of AHC or had significant phenotypic overlap. An additional case of a rare de novo variant in *RHOBTB2* was later reported in another case with an AHC-like presentation [10].

In addition to identifying variants in known genes (*ATP1A2* and *RHOBTB2*), we also identified a rare de novo in-frame indel variant

in *SCN2A*. While de novo *SCN2A* mutations have been reported extensively in neurodevelopmental disorders that sometimes include movement disorders including dystonia and episodic ataxia [2, 26, 27], we are the first to report a case that meets the AHC diagnostic criteria. Follow-up investigations identified two additional *ATP1A3*-negative typical AHC cases who were found to have a likely pathogenic *SCN2A* de novo variant in a parallel sequencing initiative. Even though the parent of origin of the other *SCN2A* variant could not be ascertained, functional data generated in this study support the variant's pathogenicity (Fig. 3).

Despite comprehensive exome sequencing, 65% ($n = 17$) of the cases studied remain genetically unexplained. These cases may be caused by variants not captured by our analyses, including non-coding variants, variants not detectable with short-read next-generation sequencing technology (complex structural rearrangements, short-tandem repeat, and copy number variants), poly- or oligogenic genetic architecture, post-zygotic events undetectable in blood, or possibly phenocopies. Future research is needed to investigate other sources of genetic variation that may explain the outstanding genetically unexplained AHC cases.

Our findings collectively suggest that some individuals with AHC or AHC-like presentations without an *ATP1A3* variant are due to genetic variants in a small number of known neurodevelopmental disease genes that have clinical presentations that have some features associated with AHC. Given the highly variable phenotypic presentation for *ATP1A3* [6, 7, 25, 28, 29] and the genetic heterogeneity observed in this study, thorough investigation of *ATP1A3* and other neurodevelopment disease genes in the clinical genetic diagnostic workup in individuals with AHC or clinical features associated with AHC is warranted.

DATA AVAILABILITY

The individuals did not consent to controlled release of the data into dbGAP or SRA, however, the raw data analyzed in this study are available from the corresponding author on reasonable request.

REFERENCES

- Verret S, Steele JC. Alternating hemiplegia in childhood: a report of eight patients with complicated migraine beginning in infancy. *Pediatrics*. 1971;47:675–80.
- Bourgeois M, Aicardi J, Goutieres F. Alternating hemiplegia of childhood. *J Pediatr*. 1993;122:673–9.

3. Mikati MA, Kramer U, Zupanc ML, Shanahan RJ. Alternating hemiplegia of childhood: clinical manifestations and long-term outcome. *Pediatr Neurol.* 2000;23:134–41.
4. Sweney MT, Silver K, Gerard-Blanluet M, Pedespan JM, Renault F, Arzimanoglou A, et al. Alternating hemiplegia of childhood: early characteristics and evolution of a neurodevelopmental syndrome. *Pediatrics.* 2009;123:e534–41.
5. Panagiotakaki E, Doummar D, Nogue E, Nagot N, Lesca G, Riant F, et al. Movement disorders in patients with alternating hemiplegia: “Soft” and “stiff” at the same time. *Neurology.* 2020;94:e1378–85.
6. Heinzen EL, Swoboda KJ, Hitomi Y, Gurrieri F, Nicole S, de Vries B, et al. De novo mutations in ATP1A3 cause alternating hemiplegia of childhood. *Nat Genet.* 2012;44:1030–4.
7. Rosewich H, Thiele H, Ohlenbusch A, Maschke U, Altmüller J, Frommolt P, et al. Heterozygous de-novo mutations in ATP1A3 in patients with alternating hemiplegia of childhood: a whole-exome sequencing gene-identification study. *Lancet Neurol.* 2012;11:764–73.
8. Swoboda KJ, Kanavakis E, Xaidara A, Johnson JE, Leppert MF, Schlesinger-Massart MB, et al. Alternating hemiplegia of childhood or familial hemiplegic migraine? A novel ATP1A2 mutation. *Ann Neurol.* 2004;55:884–7.
9. Huang D, Liu M, Wang H, Zhang B, Zhao D, Ling W, et al. De novo ATP1A2 variants in two Chinese children with alternating hemiplegia of childhood upgraded the gene-disease relationship and variant classification: a case report. *BMC Med Genom.* 2021;14:95.
10. Defo A, Verloes A, Elenga N. Developmental and epileptic encephalopathy related to a heterozygous variant of the RHOBTB2 gene: A case report from French Guiana. *Mol Genet Genom Med.* 2022;10:e1929.
11. Zagaglia S, Steel D, Krithika S, Hernandez-Hernandez L, Custodio HM, Gorman KM, et al. RHOBTB2 mutations expand the phenotypic spectrum of alternating hemiplegia of childhood. *Neurology.* 2021;96:e1539–50.
12. DePristo MA, Banks E, Poplin R, Garimella KV, Maguire JR, Hartl C, et al. A framework for variation discovery and genotyping using next-generation DNA sequencing data. *Nat Genet.* 2011;43:491–8.
13. Cingolani P, Platts A, Wang Le L, Coon M, Nguyen T, Wang L, et al. A program for annotating and predicting the effects of single nucleotide polymorphisms, SnpEff: SNPs in the genome of *Drosophila melanogaster* strain w1118; iso-2; iso-3. *Fly.* 2012;6:80–92.
14. Ren A, Zhang D, Tian Y, Cai P, Zhang T, Hu QN. Transcriptor: a comprehensive platform for annotation of the enzymatic functions of transcripts. *Bioinformatics.* 2021;37:434–5.
15. Richards S, Aziz N, Bale S, Bick D, Das S, Gastier-Foster J, et al. Standards and guidelines for the interpretation of sequence variants: a joint consensus recommendation of the American College of Medical Genetics and Genomics and the Association for Molecular Pathology. *Genet Med.* 2015;17:405–24.
16. Castro MJ, Nunes B, de Vries B, Lemos C, Vanmolkot KR, van den Heuvel JJ, et al. Two novel functional mutations in the Na⁺,K⁺-ATPase alpha2-subunit ATP1A2 gene in patients with familial hemiplegic migraine and associated neurological phenotypes. *Clin Genet.* 2008;73:37–43.
17. Pressley TA. Phylogenetic conservation of isoform-specific regions within alpha-subunit of Na⁽⁺⁾-K⁽⁺⁾-ATPase. *Am J Physiol.* 1992;262:C743–51.
18. Jiang Y, Han Y, Petrovski S, Owzar K, Goldstein DB, Allen AS. Incorporating functional information in tests of excess de novo mutational load. *Am J Hum Genet.* 2015;97:272–83.
19. Moya-Mendez ME, Mueller DM, Pratt M, Bonner M, Elliott C, Hunanyan A, et al. Early onset severe ATP1A2 epileptic encephalopathy: clinical characteristics and underlying mutations. *Epilepsy Behav.* 2021;116:107732.
20. Panagiotakaki E, Papadopoulou MT, Lesca G, Arzimanoglou A, Mikati MA. De novo mutations in CLDN5: alternating hemiplegia of childhood or not? *Brain.* 2023;146:e57–8.
21. Bassi MT, Bresolin N, Tonelli A, Nazos K, Crippa F, Baschiroto C, et al. A novel mutation in the ATP1A2 gene causes alternating hemiplegia of childhood. *J Med Genet.* 2004;41:621–8.
22. De Fusco M, Marconi R, Silvestri L, Atorino L, Rampoldi L, Morgante L, et al. Haploinsufficiency of ATP1A2 encoding the Na⁺/K⁺ pump alpha2 subunit associated with familial hemiplegic migraine type 2. *Nat Genet.* 2003;33:192–6.
23. Pietrobon D. Familial hemiplegic migraine. *Neurotherapeutics.* 2007;4:274–84.
24. de Vries B, Stam AH, Beker F, van den Maagdenberg AM, Vanmolkot KR, Laan L, et al. CACNA1A mutation linking hemiplegic migraine and alternating hemiplegia of childhood. *Cephalalgia.* 2008;28:887–91.
25. Mikati MA, Panagiotakaki E, Arzimanoglou A. Revision of the diagnostic criteria of alternating hemiplegia of childhood. *Eur J Paediatr Neurol.* 2021;32:A4–A5.
26. Ogiwara I, Ito K, Sawaiishi Y, Osaka H, Mazaki E, Inoue I, et al. De novo mutations of voltage-gated sodium channel alpha gene SCN2A in intractable epilepsies. *Neurology.* 2009;73:1046–53.
27. Wolff M, Johannesen KM, Hedrich UBS, Masnada S, Rubboli G, Gardella E, et al. Genetic and phenotypic heterogeneity suggest therapeutic implications in SCN2A-related disorders. *Brain.* 2017;140:1316–36.
28. Mikati MA, Maguire H, Barlow CF, Ozelius L, Breakefield XO, Klauck SM, et al. A syndrome of autosomal dominant alternating hemiplegia: clinical presentation mimicking intractable epilepsy; chromosomal studies; and physiologic investigations. *Neurology.* 1992;42:2251–7.
29. Rosewich H, Ohlenbusch A, Huppke P, Schlotawa L, Baethmann M, Carrilho I, et al. The expanding clinical and genetic spectrum of ATP1A3-related disorders. *Neurology.* 2014;82:945–55.
30. Rui H, Artigas P, Roux B. The selectivity of the Na⁽⁺⁾/K⁽⁺⁾-pump is controlled by binding site protonation and self-correcting occlusion. *Elife.* 2016;5:e16616.

ACKNOWLEDGEMENTS

We greatly acknowledge the subjects who participated in this study. We also thank Jean-Marc DeKeyser and Tatiana Abramova for generating and expressing the *SCN2A* variants. Moreover, we thank Geert van Weelden and Jeroen van den Heuvel for their help with the functional analysis of the *ATP1A2* variants.

AUTHOR CONTRIBUTIONS

EP, FDT, MAM, FG, AMJMvdM and ELH conceived and designed the study. EP, FDT, MAM, AVEH, LSV, FG, AMJMvdM and ELH drafted or revised the manuscript. EP, FDT, MAM, LSV, SN, AVEH, NMW, FG, AMJMvdM, and ELH generated and interpreted sequence data. CHT, ALG and JK generated and interpreted the functional data. EP, MAM, SN, GL, EA, AN, LDP, NMW, EDG, ALP, VDP, AL, MCN, AA and RV provided patient samples, phenotypic data, and interpreted genotype-phenotype correlations. All authors reviewed and approved the final version and agreed to be accountable for all aspects of the work.

FUNDING

Genetic studies were funded in part by a grant from Cure AHC (ELH), AFM-Telethon, and AFHA (SN). Functional studies of *SCN2A* were supported by NIH grant NS108874 (ALG). The variant analysis of *SCN2A* Italian patients was supported by AISEA (FG, FDT).

COMPETING INTERESTS

ALG serves on a scientific advisory board for Tevard Biosciences, and consults for Praxis Precision Medicines. ALG receives grant funding from Tevard Biosciences, Praxis Precision Medicines, and Neurocrine Biosciences for unrelated work. AMJMvdM received funding from Schedule 1 Therapeutics and Praxis Precision Medicines for unrelated work. The other authors declare no conflicts of interest.

ETHICAL APPROVAL

All subjects were consented to participate in this research study through protocols approved by local ethics boards.

ADDITIONAL INFORMATION

Supplementary information The online version contains supplementary material available at <https://doi.org/10.1038/s41431-023-01489-4>.

Correspondence and requests for materials should be addressed to Arn M. J. M. van den Maagdenberg or Erin L. Heinzen.

Reprints and permission information is available at <http://www.nature.com/reprints>

Publisher's note Springer Nature remains neutral with regard to jurisdictional claims in published maps and institutional affiliations.

Springer Nature or its licensor (e.g. a society or other partner) holds exclusive rights to this article under a publishing agreement with the author(s) or other rightsholder(s); author self-archiving of the accepted manuscript version of this article is solely governed by the terms of such publishing agreement and applicable law.